

Numerical Investigations of Turbulent Free Surface Flows Using TOPUS Scheme and Realizable Reynolds Stress Algebraic Model

Rafael Alves Bonfim de Queiroz,

Depto de Ciências de Computação, ICE, UFJF,
36036-330, Juiz de Fora, MG
E-mail: rafael.bonfim@ice.ufjf.br.

Abstract: *In this paper, it is employed the TOPUS scheme and the realizable Reynolds stress algebraic equation model for simulation of 2D incompressible turbulent free surface flows. The Reynolds averaged Navier-Stokes equations and continuity equations are solved by using the finite difference methodology on a staggered grid system. The numerical method is an adaptation of the SMAC methodology for calculating free surface fluid flows at high Reynolds numbers. The method is investigated in two types of free surface flows, namely: a turbulent free jet impinging onto flat surface and a broken dam.*

Keywords: *averaged Navier-Stokes, turbulent free surface flow, TOPUS scheme*

1 Introduction

Concerning investigations of complex free surface flows, considerable progress has currently done in the application of both finite difference method and high order upwinding (see, for example, Ferreira et al. [3, 4, 5]). In particular, the high order boundedness upwind advection scheme, called TOPUS (Third-Order Polynomial Upwind Scheme), by Queiroz et al. [13] is applied, in conjunction with the realizable Reynolds stress algebraic equation model proposed by Shih et al. [15], in an attempt of simulating incompressible turbulent free surface flows. This combination has been little investigated in the literature for high Reynolds turbulent free surface flows. This constitutes the motivation for the present study.

The basic idea underlying the TOPUS scheme is to derive a fourth degree polynomial using the recommendations of Leonard [9]. More generally, in a uniform grids, this scheme determines a family of third order accurate polynomial upwinding for computing predominantly convective flows. The derivation of the scheme is based on NVD (Normalized Variable Diagram) restrictions [9], and the TVD (Total Variation Diminishing) constraints [7]. Consequently, it satisfies the CBC (Convection-Boundedness Criterion) [6].

For simulation of free surface flows, the Reynolds averaged Navier-Stokes equations and continuity equations are solved by using the finite difference methodology on a staggered grid system, and the numerical procedure is an adaptation of the explicit SMAC (Simplified Marker-And-Cell) methodology [1] for calculating free surface fluid flows at high Reynolds numbers. The calculations are performed using the 2D version of the Freeflow simulation system [2] equipped with the TOPUS scheme and the realizable Reynolds stress algebraic equation model. Numerical experiments confirm the ability of the combination TOPUS/realizable Reynolds stress algebraic equation model for solving complex free surface flows.

It is described the fundamental equations and mathematical formulation of the TOPUS scheme in Section 2. In Section 3, two 2D numerical examples are performed for the verification/validation of the present numerical method. Conclusions are presented in Section 4.

2 Mathematical Modeling

2.1 Reynolds averaged Navier-Stokes and continuity equations

The general mathematical equations that model transient Newtonian incompressible turbulent flows are Reynolds averaged Navier-Stokes and mass conservation equations, respectively, that is

$$\frac{\partial u_i}{\partial t} + \frac{\partial(u_i u_j)}{\partial x_j} = -\frac{\partial p}{\partial x_i} + \frac{1}{Re} \frac{\partial}{\partial x_j} \left(\frac{\partial u_i}{\partial x_j} \right) - \frac{\partial(\overline{u_i u_j})}{\partial x_j} + \frac{1}{Fr^2} g_i, \quad i = 1, 2. \quad (1)$$

$$\frac{\partial u_i}{\partial x_i} = 0, \quad (2)$$

where u_i are the mean velocity components ($i = 1, 2$), p is the mean the pressure, g_i is the gravitational acceleration components, and $\overline{u_i u_j}$ is the turbulent stress tensor which it is modeled, in this study, by using realizable Reynolds algebraic equation model. The non-dimensional parameters $Re = (LU)/\nu$ and $Fr = U/(\sqrt{L|g|})$ are, respectively, the Reynolds and Froude numbers, in which L is length scale, U is characteristic velocity and ν is kinematic viscosity coefficient (constant) of the fluid. Together with appropriate boundary and initial conditions, the Eqs. (1) and (2) are solved by using the finite difference method implemented in the 2D version of the Freeflow code [2]. This code uses an explicit version of the SMAC method [1]. The details of the discretization procedure have been presented by Ferreira et al. [3].

2.2 Realizable Reynolds algebraic equation model

The turbulent stress tensor is modeled by realizable Reynolds algebraic equation model as [15]

$$\begin{aligned} \overline{u_i u_j} = & \frac{2}{3} \kappa \delta_{ij} - \nu_t \left(\frac{\partial u_i}{\partial x_j} + \frac{\partial u_j}{\partial x_i} \right) + \frac{C_{\tau 1}}{A_2 + \eta^3} \frac{\kappa^3}{\epsilon^2} \left(\frac{\partial u_i}{\partial x_k} \frac{\partial u_k}{\partial x_j} + \frac{\partial u_j}{\partial x_k} \frac{\partial u_k}{\partial x_i} - \frac{2}{3} \left(\frac{\partial u_i}{\partial x_j} \frac{\partial u_j}{\partial x_i} \right) \delta_{ij} \right) \\ & + \frac{C_{\tau 2}}{A_2 + \eta^3} \frac{\kappa^3}{\epsilon^2} \left(\frac{\partial u_i}{\partial x_k} \frac{\partial u_j}{\partial x_k} - \frac{1}{3} \left(\frac{\partial u_i}{\partial x_j} \right)^2 \delta_{ij} \right) + \frac{C_{\tau 3}}{A_2 + \eta^3} \frac{\kappa^3}{\epsilon^2} \left(\frac{\partial u_k}{\partial x_i} \frac{\partial u_k}{\partial x_j} - \frac{1}{3} \left(\frac{\partial u_i}{\partial x_j} \right)^2 \delta_{ij} \right), \end{aligned} \quad (3)$$

where δ_{ij} is the Kronecker delta and η represents the effect of the mean strain rate (denoted by S_{ij}) as

$$\eta = \frac{\kappa}{\epsilon} \sqrt{2S_{ij}S_{ij}}, \quad (4)$$

$$S_{ij} = \frac{1}{2} \left(\frac{\partial u_i}{\partial x_j} + \frac{\partial u_j}{\partial x_i} \right). \quad (5)$$

In Eq. (4), the turbulent kinetic energy κ and its dissipation rate ϵ are determined by using the two transport equations in the standard κ - ϵ model [18]:

$$\frac{\partial \kappa}{\partial t} + \frac{\partial(u_j \kappa)}{\partial x_j} - \frac{1}{Re} \left(1 + \frac{\nu_t}{\sigma_\kappa} \right) \frac{\partial}{\partial x_j} \left(\frac{\partial \kappa}{\partial x_j} \right) = P - \epsilon, \quad (6)$$

$$\frac{\partial \epsilon}{\partial t} + \frac{\partial(u_j \epsilon)}{\partial x_j} - \frac{1}{Re} \left(1 + \frac{\nu_t}{\sigma_\epsilon} \right) \frac{\partial}{\partial x_j} \left(\frac{\partial \epsilon}{\partial x_j} \right) = C_1 \frac{\epsilon}{\kappa} P - C_2 \frac{\epsilon^2}{\kappa}, \quad (7)$$

where

$$\nu_t = C_\mu \frac{\kappa^2}{\epsilon}, \quad C_\mu = \frac{2/3}{A_1 + \eta + \alpha_1 \xi}, \quad (8)$$

$$P = -\overline{u_i u_j} \frac{\partial u_i}{\partial x_j}, \quad j = 1, 2. \quad (9)$$

The parameter ξ represents the effect of the rotation rate (denoted by $\Omega_{i,j}$) as

$$\xi = \frac{\kappa}{\epsilon} \sqrt{2\Omega_{ij}\Omega_{ij}}, \quad (10)$$

$$\Omega_{ij} = \frac{1}{2} \left(\frac{\partial u_i}{\partial x_j} - \frac{\partial u_j}{\partial x_i} \right). \quad (11)$$

The coefficients C_1, C_2, σ_κ and σ_ϵ assume their standard values:

$$C_1 = 1.44, \quad C_2 = 1.92, \quad \sigma_\kappa = 1, \quad \sigma_\epsilon = 1.3, \quad (12)$$

and the additional coefficients adopted in this work are

$$C_{\tau 1} = -4, \quad C_{\tau 2} = 13, \quad C_{\tau 3} = -2, \quad A_1 = 5000, \quad A_2 = 1000, \quad \alpha_1 = 0. \quad (13)$$

It is important to inform to the reader that Shih et al. [15] recommend that the adjustable constants $A_1, A_2, C_{\tau 1}, C_{\tau 2}$ and $C_{\tau 3}$ must satisfy: $A_1 > 0, A_2 > 0$ and $2C_{\tau 1} + C_{\tau 2} + C_{\tau 3} > 0$.

2.3 Initial and boundary conditions

Equations (1), (2), (6) and (7) are coupled non-linear PDEs and are sufficient, in principle, to solve for the unknowns u_i, p, κ and ϵ when appropriate initial and boundary conditions are specified. In this study, a staggered grid is used where the p, κ and ϵ are stored at the centre of a computational grid cell, while u_i are stored at the cell edges. With this grid system, p boundary conditions are not needed. The boundary and initial conditions have been implemented as follows.

For initial conditions, u_i and p are specified in the same way as in the laminar case [16]; that is, these variables are prescribed. The initial conditions for κ and ϵ are adopted as functions of an upstream turbulent intensity I [18]. In non-dimensional form, the κ and ϵ are estimated by, respectively, as

$$\kappa = IRe, \quad \epsilon = \frac{\kappa}{\beta} \sqrt{\frac{\kappa}{Re}}, \quad (14)$$

where the values $I = 0.08$ and $\beta = 0.01$ were employed.

Four types of boundary conditions have been implemented, namely: inflow, outflow, rigid-wall and free surfaces boundaries. At the inflow, the velocities u_i are prescribed while the values of κ and ϵ are estimated in such a way that they are consistent with the initial conditions (14). At the outflow, the streamwise gradient for each variable is required to be equal to zero (homogeneous Neumann conditions). At free surface, the normal and tangential components of the stress must be continuous across any free surface; hence on such a surface has been (see Ferreira et al. [3] for details)

$$\mathbf{n} \cdot \boldsymbol{\sigma} \cdot \mathbf{n} = 0, \quad (15)$$

$$\mathbf{m} \cdot \boldsymbol{\sigma} \cdot \mathbf{n} = 0, \quad (16)$$

where \mathbf{n} is the local unit normal vector, external to the free surface, and \mathbf{m} is the local tangent vector to the free surface and tensor $\boldsymbol{\sigma}$ adopted in this study is given by

$$\sigma_{ij} = - \left(p + \frac{2}{3}\kappa \right) \delta_{ij} + \frac{(1 + \nu_t)}{Re} \left(\frac{\partial u_i}{\partial x_j} + \frac{\partial u_j}{\partial x_i} \right). \quad (17)$$

From condition (15) one determines the pressure; and from (16) one obtains the velocities at the free surface. The turbulent variables at the free surface are determined by imposing

$$\frac{\partial \kappa}{\partial n} = 0, \quad \frac{\partial \epsilon}{\partial n} = 0. \quad (18)$$

The boundary conditions at a rigid-wall are based on the wall function approach. The equation for determining the turbulent variables near a rigid wall is the total wall shear stress τ_w given by [18]

$$u_\tau^2 = \tau_w, \tag{19}$$

where u_τ is the friction velocity. The values of the κ and ϵ in the inertial sublayer are, respectively, prescribed by the relations [18]

$$\kappa = \frac{Re\tau_w}{\sqrt{C_\mu}}, \quad \epsilon = \frac{Re\tau_w u_\tau}{\mathbf{K}z_w}, \tag{20}$$

where $\mathbf{K} = 0.41$ is the von Kármán constant [12]. In the viscous sublayer, it is used the strategy of Sondak and Pletcher [14]; that is,

$$\kappa = Re \frac{\tau_w}{\sqrt{C_\mu}} \left(\frac{z^+}{z_c^+} \right)^2, \quad \epsilon = \frac{\kappa}{l^*} \sqrt{\frac{\kappa}{Re}}, \tag{21}$$

where z^+ is defined as $z^+ = Reu_\tau z_w$, and l^* represents the length scale proposed by Norris and Reynolds [11]. The critical value of z^+ (denoted by z_c^+) is solution of the following equation:

$$\ln(Ez_c^+) - \mathbf{K}z_c^+ = 0, \tag{22}$$

where $E = \exp(\mathbf{K}B)$; B is an empirical constant, whose value is between 5.0 and 5.2 for Newtonian fluid.

2.4 TOPUS scheme

The philosophy of the TOPUS scheme for convective terms discretization constructed is to define a fourth degree polynomial that passes through the $O(0, 0)$, $Q(0.5, 0.75)$ and $P(1, 1)$ critical points into the CBC region, and that it contains a free parameter α in its formulation. In short, in normalized variable (NV), the general TOPUS scheme can be defined as [4, 13]

$$\hat{\phi}_f = \begin{cases} \alpha \hat{\phi}_U^4 + (-2\alpha + 1) \hat{\phi}_U^3 + \left(\frac{5\alpha-10}{4}\right) \hat{\phi}_U^2 + \left(\frac{-\alpha+10}{4}\right) \hat{\phi}_U, & \hat{\phi}_U \in [0, 1], \\ \hat{\phi}_U, & \hat{\phi}_U \notin [0, 1], \end{cases} \tag{23}$$

where $-2 \leq \alpha \leq 2$ ensures that the TOPUS scheme satisfies the CBC criterion and $\hat{\phi}_U = \frac{\phi_U - \phi_R}{\phi_D - \phi_R}$ is the NV of Leonard [9]. The neighboring nodes D (Downstream), U (Upstream) and R (Remote-upstream) of a face f are defined according to velocity V_f at this face (see [4, 13] for details). In this work, the TOPUS scheme is used with $\alpha = 2$. In this case, it is entirely contained in the TVD region [7].

3 Numerical experiments

A combination of TOPUS scheme and realizable Reynolds stress algebraic equation model for simulating 2D high Reynolds incompressible turbulent flows is assessed in this section. Verification is made against a turbulent jet impinging onto a flat surface and validation is made against the broken dam problem. These problems were selected because there are analytical and experimental data available in the literature.

3.1 Turbulent free jet impinging onto a rigid wall

The first result is a 2D jet impinging normally onto flat surface at high Reynolds number. This free surface flow in turbulent regime has been chosen as a representative test case because there is (see [17]) an analytical solution for the total thickness of the fluid layer flowing on the flat rigid

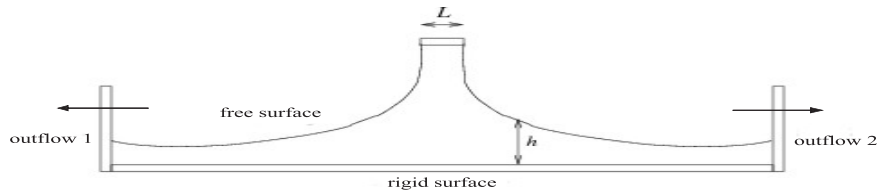


Figure 1: Configuration of a free jet impinging onto a rigid surface.

wall. It is difficult to simulate because the free surface boundary conditions must be specified on an arbitrarily moving boundary (see an illustration in Fig. 1).

The numerical solver simulated this problem at Reynolds number (Re) 5.0×10^4 , which was based on the maximum velocity $U_{max} = 1.0$ m/s and diameter of the inlet $L = 0.01$ m. Three meshes were used, namely: the coarse mesh 200×50 ($\delta_x = \delta_y = 0.001$ m); the medium mesh 400×100 ($\delta_x = \delta_y = 0.0005$ m); and the fine mesh 800×200 ($\delta_x = \delta_y = 0.00025$ m) computational cells. By using these meshes, a comparison was made between the free surface height (the total thickness of the layer), obtained from numerical method and from the analytical viscous solution [17]. This is displayed in Fig. 2. One can see from this figure that the numerical results on fine mesh are generally in good agreement with the analytical solution, displaying small differences in some regions of the flow. This difference may be attributed to insufficient grid points used near the rigid wall.

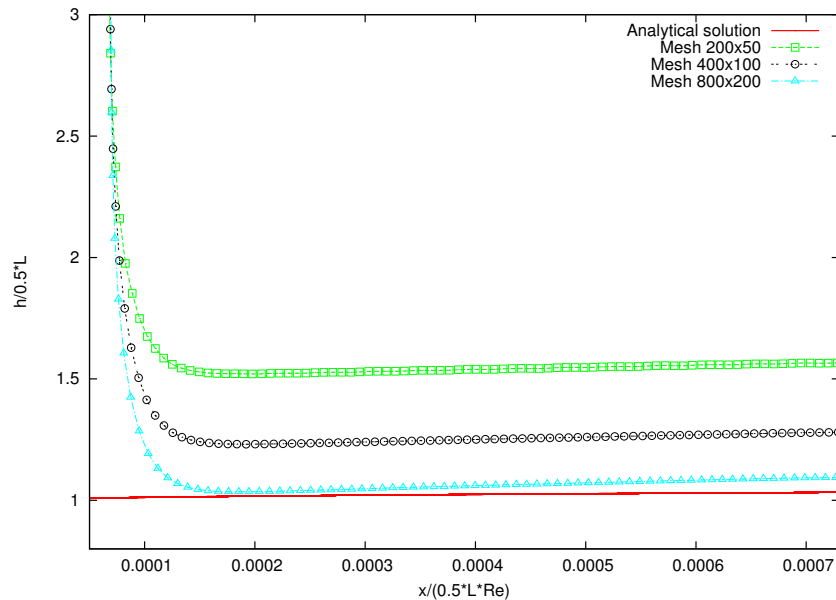


Figure 2: Comparison on three meshes between numerical solution and analytical solution.

3.2 Broken dam problem

Results are presented now for the collapse of a column of water onto a horizontal wall for 2D case. This free surface flow problem was first studied experimentally in detail by Martin and Moyce [10], and more recently by Koshizuka and Oka [8] to investigate the spreading velocity and the falling rate of water columns. It is performed the simulation of this unsteady free surface flow. The geometry used is a fluid column ($a = 0.05$ m wide and $2a = 0.1$ m high) in hydrostatic equilibrium and confined between walls. At the beginning, a wall is instantaneously removed and the fluid is subject to vertical gravity and it is free to flow out along a rigid horizontal wall. In order to compare with the experimental data [8, 10], the free-slip boundary condition was

used to correctly model the flow at walls. The Reynolds number based on the characteristic length $L = 2a$ and the characteristic velocity $U = \sqrt{L|\mathbf{g}|}$ was $Re \approx LU/\nu = 99 \times 10^3$ ($|\mathbf{g}| = 9.81\text{ms}^{-2}$). The mesh used in this problem was: 150×75 ($\delta_x = \delta_y = 0.002$ m) computational cells.

Figure 3 shows the 2D numerical results and experimental data for the positions of the fluid front (x_{max}) versus time. As shown in this figure, calculations agree fairly well with the experimental data specially in the comparison with the results of Martin and Moyce, giving confidence in the numerical solutions.

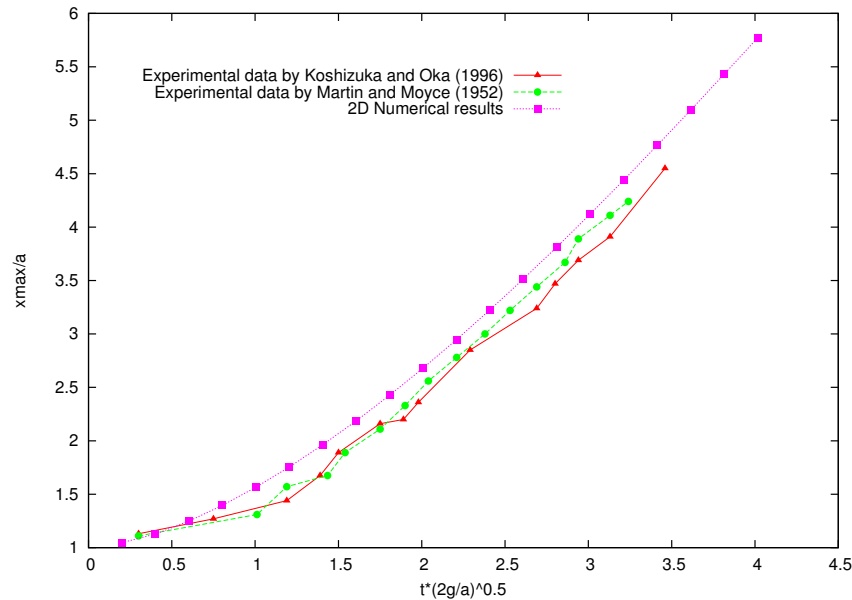


Figure 3: Comparison between present computations and experimental data for the surge front position x_{max} versus non dimensional time.

4 Conclusion

A combination of TOPUS scheme and realizable Reynolds stress algebraic equation model has been applied for the numerical simulation of incompressible turbulent free surface flows. It provided numerical results in good agreement with existing analytical and experimental data available in the literature.

5 Acknowledgment

This research work was supported by the *FAPESP* under Grant 06/05910-1.

References

- [1] A. A. Amsden and F. H. Harlow, A simplified MAC technique for incompressible fluid flow calculations, *J. Compu. Phys.*, 6 (1971) 322-325.
- [2] A. Castello F., M. F. Tomé, C. N. L. César, S. McKee, J.A. Cuminato, Freeflow: an integrated simulation system for three-dimensional free surface flows, *Comput. Visualization in Science*, 2 (2000) 199-210.

- [3] V. G. Ferreira, C. M. Oishi, F. A. Kurokawa, M. K. Kaibara, J. A. Cuminato, A. Castelo, N. Mangiavacchi, M. F. Tomé, S. McKee, A combination of implicit and adaptative upwind tools for the numerical solution of incompressible free surface flows, *Commun. Numer. Meth. En.*, 23 (2007) 419-445.
- [4] V. G. Ferreira, R. A. B. Queiroz, G. A. B. Lima, R. G. Cuenca, C. M. Oishi, J. L. F. Azevedo, S. McKee, A bounded upwinding scheme for computing convection-dominated transport problems, *Comput. Fluids*, 57 (2012) 208–224.
- [5] V. G. Ferreira, R. A. B. Queiroz, M. A. C. Candemazo, G. A. B. Lima, L. Corrêa, C. M. Oishi, F. L. P. Santos, Simulation results and applications of an advection bounded scheme to practical flows, *Comp. Appl. Math.*, 31 (2012) 591–616.
- [6] P. H. Gaskell, A. K. C. Lau, Curvature-compensated convective transport: SMART, a new boundedness-preserving transport algorithm, *Int. J. Numer. Methods Fluids*, 8 (1988) 617-641.
- [7] A. Harten, High resolution schemes for conservation laws, *J. Compu. Phys.*, 49 (1983) 357-393.
- [8] S. Koshizuka, Y. Oka, Moving-particle semi-implicit method for fragmentation of incompressible fluids, *Nucl. Sci. Eng.*, 123 (1996) 421-434.
- [9] B. P. Leonard, Simple high-accuracy resolution program for convective modeling of discontinuities, *Int. J. Numer. Methods Fluids*, 8 (1988) 1291–1318.
- [10] J. C. Martin, W. J. Moyce, An experimental study of the collapse of liquid columns on a rigid horizontal plate, *Phil Trans Math Phys Eng Sci*, 244 (1952) 312–324.
- [11] H. L. Norris, W. C. Reynolds, Turbulent channel flow with a moving wavy boundary, Stanford Univ. Dept. Mech. Eng. TR TF-7, 1975.
- [12] V. C. Patel, Perspective: flow at high Reynolds number and over rough surfaces-Achilles Heel of CFD, *J. Fluids Eng.*, 120 (1998) 434–444.
- [13] R. A. B. Queiroz, V. G. Ferreira, “Development and testing of high-resolution upwind schemes: Upwind schemes for incompressible free surface flows”, VDM Verlag Dr. Muller, Alemanha, 2010.
- [14] D. L. Sondak, R. H. Pletcher, Application of wall functions to generalized nonorthogonal curvilinear coordinate systems, *AIAA Journal*, 33 (1995) 33–41.
- [15] T.-H. Shih, J. Zhu, J. L. Lumley, A realizable Reynolds stress algebraic equation model, Lewis Research Center, 1993.
- [16] M. F. Tomé, A. Castelo, J. Murakami, J. A. Cuminato, R. Minghim, M. C. F. Oliveira, N. Mangiavacchi, S. McKee, Numerical simulation of axisymmetric free surface flows, *J. Compu. Phys.*, 157 (2000) 441-472.
- [17] E. J. Watson, The radial spread of a liquid jet over a horizontal plane, *J. Fluid Mech*, 20 (1964) 481–499.
- [18] D. C. Wilcox, “Turbulence modeling for CFD”, D C W Industries, 2006.